Intramolecular and Intermolecular Bonding in Benzene Cluster Isomers

Dario Braga,*[1a] Paul J. Dyson,[1b] Fabrizia Grepioni,[1a] Brian F. G. Johnson,[1b] and Maria José Calhorda*[1c]

Dipartimento di Chimica G. Ciamician, Università di Bologna, Via Selmi 2, 40126 Bologna, Italy, Department of Chemistry, The University of Edinburgh, West Mains Road, Edinburgh, U.K., Instituto de Tecnologia Química e Biológica, R. da Quinta Grande 6, 2780 Oeiras, Portugal, and Instituto Superior Técnico, Lisboa, Portugal

Received February 9, 1994®

The bonding in the prototypical high-nuclearity arene cluster complexes $Ru_5C(CO)_{12}(C_6H_6)$ and $Ru_6C(CO)_{11}(C_6H_6)_2$ has been investigated using extended Hückel calculations. The relative stability of the known isomeric pairs $Ru_5C(CO)_{12}(\eta^6\text{-}C_6H_6)$ and $Ru_5C(CO)_{12}(\mu_3\text{-}\eta^2\text{:}\eta^2\text{:}\eta^2\text{-}C_6H_6)$, $Ru_6C(CO)_{11}(\eta^6\text{-}C_6H_6)_2$ and $Ru_6C(CO)_{11}(\eta^6\text{-}C_6H_6)(\mu_3\text{-}\eta^2\text{:}\eta^2\text{:}\eta^2\text{-}C_6H_6)$ has been related to the chemically characterized interconversion process occurring in solution. Attention has been focused on the relationship between the apical (η^6) and facial ($\mu_3\text{-}\eta^2\text{:}\eta^2\text{:}\eta^2$) bonding modes of benzene with the central cluster unit. The calculations lead to the conclusion that the apical isomers are the more stable, although the local benzene–ruthenium interaction is stronger in the facial isomers. The molecular organization in the respective crystal structures as well as the relative cohesion of the solid materials has been investigated by empirical packing potential energy calculations. The relationship between stability of the individual arene cluster *molecules* and that of the same *molecules in the solid state* has been addressed in terms of the relative crystal cohesion. Hydrogen bonds of the C–H··O–C type have been detected in crystals of the apical isomers. In crystalline *trans*-$Ru_6C(CO)_{11}(\eta^6\text{-}C_6H_6)_2$ molecular piles are formed by molecules joined by direct benzene–benzene interactions; a similar packing motif is also present in crystalline $Ru_6C(CO)_{11}(\eta^6\text{-}C_6H_6)(\mu_3\text{-}\eta^2\text{:}\eta^2\text{:}\eta^2\text{-}C_6H_6)$.

Introduction

The chemistry of arene carbonyl clusters has been extensively investigated over the last few years, and within this family of complexes the clusters synthesized and structurally characterized in both solution and the solid state are diverse.[2] Clusters of nuclearity between three and eight are known in which one or more arene ligands are present. Given the same metallic core, the main structural difference between them arises from the bonding mode adopted by the arenes. The prototypes of these molecules are benzene derivatives. For benzene essentially two different bonding modes have been observed directly, namely the apical bonding mode (η^6-coordination), in which the carbon atoms of the benzene ring interact with a single metal center, and the facial bonding mode ($\mu_3\text{-}\eta^2\text{:}\eta^2\text{:}\eta^2$-coordination), in which benzene interacts with three metal atoms forming a triangle. In this latter coordination geometry the midpoints of alternating C–C bonds around the ring are eclipsed, or very nearly so, with the metal atoms. The facial bonding has been the subject of extensive structural and spectroscopic investigation and is found in ruthenium and osmium clusters of nuclearities three, five, and six. This mode of bonding has been observed also in the cobalt derivatives of the type $(CpCo)_3(\mu_3\text{-}\eta^2\text{:}\eta^2\text{:}\eta^2\text{-}trans\text{-}\beta\text{-}$methylstyrene).[2b] Adsorption of benzene on several metallic surfaces under ultra-high vacuum conditions have also revealed the same facial coordination mode.[2c]

Most arene clusters have been characterized by single crystal X-ray diffraction experiments in the solid state. The molecular structures of these complexes present some intriguing aspects arising from the availability of different coordination sites on the metal framework as well as from the different bonding modes available to the arene ligands. This gives rise to the presence of structural isomers which differ in site and type of coordination. In square-pyramidal pentaruthenium arene clusters, for instance, the arene can bind either apically, to one of the four basal atoms of the cluster, or to its vertex; facial bonding is also possible on one of the cluster triangular faces. Similar isomery is possible in hexanuclear octahedral clusters. The number of possible isomers increases when more than one arene is coordinated. In ruthenium clusters of nuclearity three, five, and six, as well in trinuclear osmium clusters, interconversion between these isomers can be induced both chemically and thermally.

It has also been shown in many instances that the molecular organization in the *crystal structure* of arene cluster complexes results from a complex optimization of the interlocking of the flat arene fragments with the other ligands present on the cluster surface, *viz.* carbon monoxide in terminal or bridging bonding geometry. In general, preferential arene–arene interactions of the graphitic type are established in crystals of bis(arene) derivatives while mono(arene) derivatives form ribbons in the so called "herring-bone" pattern.[4]

The molecular chemistry of clusters containing benzene in the facial mode has provided model systems for the interaction of arene molecules with metallic surfaces. New insight into chemisorption phenomena has been provided in keeping with early suggestions that metal clusters could represent a bridge between material and molecular chemistry.[5]

* Abstract published in *Advance ACS Abstracts*, June 1, 1994.

(1) (a) University of Bologna. (b) University of Edinburgh. (c) Instituto Superiore Tecnico of Lisbon and CTQB (Oeiras).

(2) (a) Braga, D.; Dyson, P. J.; Grepioni, F.; Johnson, B. F. G. *Chem. Rev.*, in press. (b) Wadepohl, H. *Angew. Chem., Int. Ed. Engl.* **1992**, *31*, 247. (c) Wadepohl, H.; Büchner, K.; Herrmann, M.; Pritzkow, H. *Organometallics* **1991**, *10*, 861.

(3) (a) Somorjai, G. A. The Building of Catalysts: A Molecular Surface Science Approach In *Catalyst Design-Progress and Perspectives*; Hegedus, L. L., Ed.; John Wiley & Sons: New York, 1987. (b) Somorjai, G. A. *Chemistry in Two Dimensions: Surfaces*; Cornell University Press: Ithaca, New York. (c) Albert, M. R.; Yates, J. T., Jr. *The Surface Scientist's Guide to Organometallic Chemistry*; American Chemical Society, Washington, DC, 1987. (d) Koel, B. E.; Somorjai, G. A. *Surface Structural Chemistry: Catalysis Science and Technology*; Anderson, J. R., Boudart, M., Eds.; Springer Verlag: Berlin, 1984.

(4) (a) Braga, D.; Grepioni, F.; Johnson, B. F. G.; Chen, H.; Lewis, J. *J. Chem. Soc., Dalton Trans.* **1991**, 2559. (b) Braga, D.; Grepioni, F.; Righi, S.; Dyson, P. J.; Johnson, B. F. G.; Bailey, P. J.; Lewis, J. *Organometallics* **1992**, *11*, 4042. (c) Braga, D.; Grepioni, F.; Righi, S; Johnson, B. F. G.; Bailey, P. J.; Dyson, P. J.; Lewis, J.; Martinelli M. *J. Chem. Soc., Dalton Trans.* **1992**, 2121.

0020-1669/94/1333-3218$04.50/0

In this article the relationship between *molecular and crystal structures* of some benzene cluster isomers is investigated. Since we are interested in the mode of bonding of benzene (and, more generally, arenes) with transition metal cluster units and in the intermolecular assembly of arene clusters in the solid state, attention will be focused on two pairs of arene cluster isomers, namely the pentanuclear species $Ru_5C(CO)_{12}(\mu_3\text{-}\eta^2\text{:}\eta^2\text{:}\eta^2\text{-}C_6H_6)$ and $Ru_5C(CO)_{12}(\eta^6\text{-}C_6H_6)$,[6] and the hexanuclear species $Ru_6C(CO)_{11}(\eta^6\text{-}C_6H_6)(\mu_3\text{-}\eta^2\text{:}\eta^2\text{:}\eta^2\text{-}C_6H_6)$ and $Ru_6C(CO)_{11}(\eta^6\text{-}C_6H_6)_2$ and on their respective crystals.[7,8] There are several reasons for choosing these isomers: (i) The solid-state molecular structures of these molecules are known to a high level of accuracy (compatible with the size of these clusters). (ii) Chemical and spectroscopic evidence provide a clear sequence of stability of the different isomers in solution. (iii) These two isomeric pairs represent effectively two rather uncommon cases in which isomers of an interconversion process have been separated and characterized independently in the solid state.

Our approach to the problems outlined above will be from two different sides: the molecular structures and the relative stability of the two types of benzene coordination modes will be investigated by extended Hückel molecular orbital calculations. Attention will also be paid to the facial–apical interconversion process occurring in solution. The crystal structures will be studied with the aid of empirical atom–atom pairwise packing potential energy calculations and computer graphics. Both methods have proved in many other instances to be capable of providing valuable insight into fundamental aspects of the structural chemistry of organometallic molecules.

To our knowledge a *combined* study of molecular and crystal features and of their inter-relationship has never been attempted before in the cluster chemistry field.

Results and Discussion

Structural Characteristics and Molecular Orbital Calculations. In this section we summarize briefly the results of previous theoretical investigations of the interaction between arenes and metal cluster of high nuclearity as well as the most relevant structural features of the complexes under discussion.

Previous theoretical work has been essentially focused on trinuclear species.[12,13]

The trinuclear complexes $M_3(CO)_9(\mu_3\text{-}\eta^2\text{:}\ \eta^2\text{:}\ \eta^2\text{-}C_6H_6)$ (M = Ru[9] and Os[10] can be regarded as the prototypical clusters in the series of face-capped $\mu_3\text{-}\eta^2\text{:}\ \eta^2\text{:}\ \eta^2$-arene species. The face-capping benzene ligand in these complexes shows an alternation of long and short bonds within the C_6 ring, the short bonds being those interacting directly with the metal atoms. In the case of $Ru_3(CO)_9(\mu_3\text{-}\eta^2\text{:}\ \eta^2\text{:}\ \eta^2\text{-}C_6H_6)$ long and short C–C bonds average 1.45(1), 1.40(2) and 1.45(1), 1.41(1) Å at room temperature and 193 K, respectively. The difference between the two sets of bonds (0.05 Å) is much smaller than that observed in the osmium complex (Δ = 0.10 Å), although the poorer quality of this latter data set makes this latter difference less significant. In the tricobalt cluster $(CpCo)_3(\mu_3\text{-}\eta^2\text{:}\eta^2\text{:}\eta^2\text{-}trans\text{-}\beta$-methylstyrene) the same distortions are apparent, but the differences even smaller (Δ = 0.03 Å).[2b,c] The deviation from the idealized D_{6h} symmetry of "free" benzene to a "Kekulé-type" structure upon face capping resembles that of the hypothetical 1,3,5-cyclohexatriene molecule. Similar distortions have been observed for benzene chemisorbed on metal atom surfaces.[11]

Direct location of the benzene H-atoms in $Ru_3(CO)_9(\mu_3\text{-}\eta^2\text{:}\ \eta^2\text{:}\ \eta^2\text{-}C_6H_6)$ allowed also for the observation of out-of-plane bending (21.1 and 21.5° at room temperature and at 193 K, respectively) of the C–H bonds away from the ruthenium atoms.[9]

The electronic bases for bonding in such complexes has been analysed *via* the Fenske–Hall quantum chemical method by using $Ru_3(CO)_9(\mu_3\text{-}\eta^2\text{:}\ \eta^2\text{:}\ \eta^2\text{-}C_6H_6)$ to model the osmium species.[9b,10] The results were consistent with the observed C–C bond length alternation and showed that the interaction between the ligand and the trimetal unit is enhanced if out-of-plane bending (away from the metal core) of the C–H bonds is allowed along with an expansion of the C_6 ring. In good agreement with the observed values, a bending of 10–20° was predicted. Displacement of hydrogen atoms from the arene plane is also commonly observed in mononuclear complexes, this displacement being either toward or away from the metal center. Hoffmann[12a] has attributed this displacement to a reorientation of the benzene molecular orbitals for more effective overlap with metal-based orbitals.

The electronic structure of tricobalt derivatives has also been investigated by Fenske–Hall quantum chemical calculations, using as a model $(CpCo)_3(\mu_3\text{-}\eta^2\text{:}\eta^2\text{:}\eta^2\text{-}C_6H_6)$, based on the solid state structure of $(CpCo)_3(\mu_3\text{-}\eta^2\text{:}\eta^2\text{:}\eta^2\text{-}trans\text{-}\beta$-methylstyrene), with the molecular symmetry idealized as C_3.[12b] Because of the isolobal relationship between CpCo and $(CO)_3Fe$ fragments, the sequence of frontier orbitals was found similar to that obtained earlier by extended Hückel molecular orbital calculations on the hypothetical complex $[(CO)_3Fe]_3(\mu_3\text{-}\eta^2\text{:}\eta^2\text{:}\eta^2\text{-}C_6H_6)]$.[12a] In $(CpCo)_3(\mu_3\text{-}\eta^2\text{:}\ \eta^2\text{:}\eta^2\text{-}C_6H_6)$ the main interaction arises from π-donation from benzene orbitals accompanied by back donation from the $(CpCo)_3$; viz., benzene acts as both a π-acceptor and a π-donor ligand.

Recently, the electronic structure of the osmium complex $Os_3(CO)_9(\mu_3\text{-}\eta^2\text{:}\eta^2\text{:}\eta^2\text{-}C_6H_6)$ has been subjected to an *ab-initio* calculation and MO analysis.[13] It has been shown that the interaction of benzene with the $Os_3(CO)_9$ fragment can be described in terms of donation and back-donation which is enhanced by CH bending.

The isomeric pair $Ru_5C(CO)_{12}(\mu_3\text{-}\eta^2\text{:}\eta^2\text{:}\eta^2\text{-}C_6H_6)$ and $Ru_5C(CO)_{12}(\eta^6\text{-}C_6H_6)$ is obtained from the cyclohexa-1,3-diene adduct $Ru_5C(CO)_{13}(\mu_2\text{-}\eta^2\text{:}\eta^2\text{-}C_6H_8)$.[6] Both clusters maintain the square-pyramidal metal framework of the precursor and of the parent molecule $Ru_5C(CO)_{15}$. The main difference between the structures of the two isomers arises from the benzene coordination as shown in Figure 1. The coordination of benzene in $Ru_5C(CO)_{12}(\mu_3\text{-}\eta^2\text{:}\eta^2\text{:}\eta^2\text{-}C_6H_6)$ is essentially of the same type as discussed previously for $Ru_3(CO)_9(\mu_3\text{-}\eta^2\text{:}\eta^2\text{:}\eta^2\text{-}C_6H_6)$ and $(CpCo)_3(\mu_3\text{-}\eta^2\text{:}\ \eta^2\text{:}\eta^2\text{-}trans\text{-}\beta$-methylstyrene). The metal atom framework in $Ru_5C(CO)_{12}(\eta^6\text{-}C_6H_6)$ is heavily distorted with respect to the geometry of $Ru_5C(CO)_{15}$. The C(carbide) atom is off-centered with respect to the middle of the square base, being closer to the Ru atom carrying the apical benzene ligand than to the other atoms [1.93(2), and 1.86(2) *versus* an average of 2.03(2), and 2.06(2) Å for the two independent molecules present in the asymmetric unit].

The η^6-terminal and $\mu_3\text{-}\eta^2\text{:}\eta^2\text{:}\eta^2$-bonding modes have also been observed in the solid state structure of arene derivatives of Ru_6C-

(5) Muetterties, E. L. *Chem. Eng. News* **1982**, *60*, 28. Muetterties, E. L. *Science* **1977**, 196, 839. Muetterties, E. L.; Rhodin, T. N.; Band, E.; Bruckner, C. F.; Pretzer, W. R. *Chem. Rev.* **1979**, *79*, 91.
(6) Braga, D.; Grepioni, F.; Sabatino, P.; Dyson, P. J.; Johnson, B. F. G.; Lewis, J.; Bailey, P. J.; Raithby, P. R.; Stalke, D. *J. Chem. Soc., Dalton Trans.* **1993**, 985.
(7) (a) Gomez-Sal, M. P.; Johnson, B. F. G.; Lewis, J.; Raithby, P. R.; Wright, A. H. *J. Chem. Soc., Chem. Commun* **1985**, 1682. (b) Dyson, P. J.; Johnson, B. F. G.; Lewis, J.; Martinelli, M.; Braga, D.; Grepioni, F. *J. Am. Chem. Soc.* **1993**, *115*, 9062.
(8) Adams, R. D.; Wu, W. *Polyhedron* **1992**, *2*, 2123.
(9) (a) Johnson, B. F. G.; Lewis, J.; Martinelli, M.; Wright A. H.; Braga, D.; Grepioni, F.; *J. Chem. Soc., Chem. Commun.* **1990**, 364. (b) Braga, D.; Grepioni, F.; Johnson, B. F. G.; Lewis, J.; Housecroft, C. E.; Martinelli, M. *Organometallics* **1991**, *10*, 1260.
(10) Gallop, M. A.; Gomez-Sal, M. P.; Housecroft, C. E.; Johnson, B. F. G.; Lewis, L.; Owen, S. M.; Raithby, P. R.; Wright, A. H. *J. Am. Chem. Soc.* **1992**, *114*, 2502.
(11) Lin, R. F.; Blackman, G. S.; VanHove, M. A.; Samorjai, G. A. *Acta Crystallogr., Sect. B* **1987**, *B43*, 368. VanHove, M. A.; VanHove, M. A.; Samorjai, G. A. *J. Am. Chem. Soc.* **1986**, *108*, 2532.
(12) (a) Pinhas, A. R.; Albright, T. A.; Hoffmann, R. *Helv. Chim. Acta* **1980**, *63*, 29. (b) Wadepohl, H.; Zhu, L. *J. Organomet. Chem.* **1989**, *376*, 115.
(13) Riehl, J. F.; Koga, N.; Morokuma, K. *Organometallics* **1993**, *12*, 4788 and references therein.

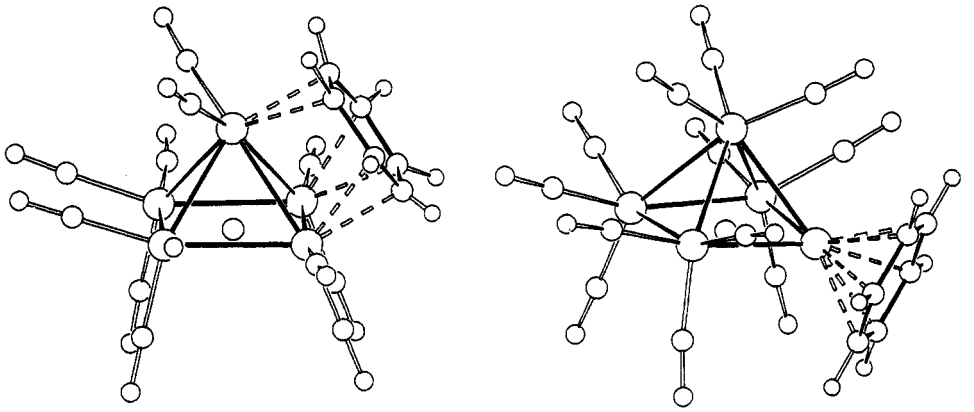

Figure 1. Molecular structures of $Ru_5C(CO)_{12}(\mu_3\text{-}\eta^2\text{:}\eta^2\text{:}\eta^2\text{-}C_6H_6)$ and $Ru_5C(CO)_{12}(\eta^6\text{-}C_6H_6)$ as obtained by single-crystal X-ray diffraction.

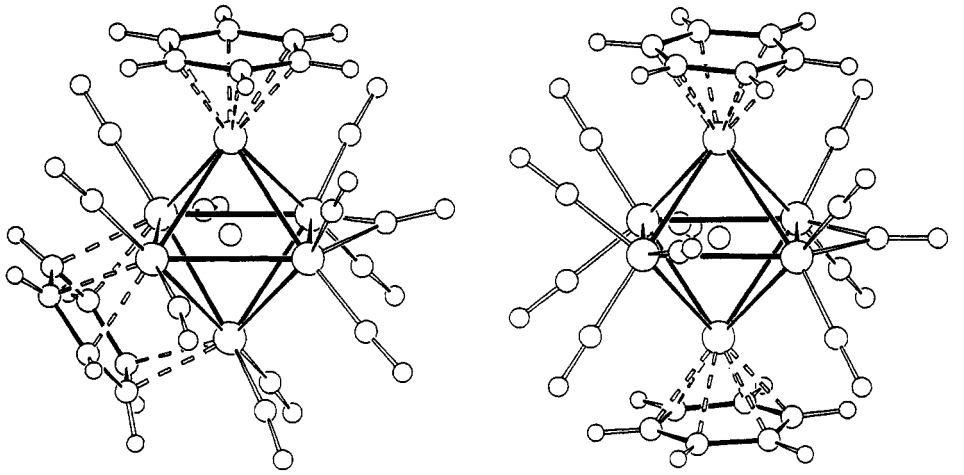

Figure 2. Molecular structures of $Ru_6C(CO)_{11}(\eta^6\text{-}C_6H_6)(\mu_3\text{-}\eta^2\text{:}\eta^2\text{:}\eta^2\text{-}C_6H_6)$ and $Ru_6C(CO)_{11}(\eta^6\text{-}C_6H_6)_2$ as obtained by single crystal X-ray diffraction.

$(CO)_{17}$.[14] Although the μ_3-coordination is characteristic of the benzene fragment, it is also adopted in two cases by substituted rings, *e.g.* by paracyclophane in $Ru_6C(CO)_{14}(\mu_3\text{-}\eta^2\text{:}\eta^2\text{:}\eta^2\text{-}C_{16}H_{16})$[15] and by toluene in $Ru_6C(CO)_{11}(\eta^6\text{-}C_6H_5Me)(\mu_3\text{-}\eta^2\text{:}\eta^2\text{:}\eta^2\text{-}C_6H_5Me)$.[16] Xylene,[15] toluene,[17a] mesitylene,[17b] and triethylbenzene[15] have only been found to adopt η^6-coordination modes. In all these derivatives the octahedral metal framework contains an interstitial carbon atom.

The low-energy CO scrambling around the metal framework in solution is reflected in an almost continuous distribution of metal–CO bonding geometries from symmetric bridges, *via* asymmetric bridging and "bent terminal", to linear terminal ligands in the solid-state structure of all mono- and bis(arene) derivatives characterized to date.

In the case of bis(arene) clusters three isomeric forms have been established. These correspond to the general formulas *trans*-$Ru_6C(CO)_{11}(\eta^6\text{-arene})_2$, *cis*-$Ru_6C(CO)_{11}(\eta^6\text{-arene})_2$, and $Ru_6C(CO)_{11}(\eta^6\text{-arene})(\mu_3\text{-}\eta^2\text{:}\eta^2\text{:}\eta^2\text{arene})$. *Trans*-$\eta^6$ isomers are known for the species $Ru_6C(CO)_{11}(\eta^6\text{-}C_6H_6)_2$[8] and $Ru_6C(CO)_{11}(\eta^6\text{-}C_6H_3Me_3)_2$.[4b] The apical–facial structural form is characteristic of the complexes of formula $Ru_6C(CO)_{11}(\eta^6\text{-arene})(\mu_3\text{-}\eta^2\text{:}\eta^2\text{:}\eta^2\text{-}C_6H_6)$ (arene = C_6H_6, C_6H_5Me, $C_6H_4Me_2$). In these complexes one of the rings adopts the η^6-apical coordination, while the other ring is bound in $\mu_3\text{-}\eta^2\text{:}\eta^2\text{:}\eta^2$-capping mode to one triangular face of the octahedral metal framework. The methyl-substituted ring always adopts the terminal coordination mode. The structures of the two isomers $Ru_6C(CO)_{11}(\eta^6\text{-}C_6H_6)_2$ and $Ru_6C(CO)_{11}(\eta^6\text{-}C_6H_6)(\mu_3\text{-}\eta^2\text{:}\eta^2\text{:}\eta^2\text{-}C_6H_6)$ are shown in Figure 2. The *cis*-η^6 form has been observed in the solid state only for the *cis*-$Ru_6C(CO)_{11}(\eta^6\text{-}C_6H_3Me_3)(\eta^6\text{-}C_6H_6)$.[4b]

Extended Hückel Calculations. We performed extended Hückel calculations[18] on these Ru_5 and Ru_6 clusters in order to gain insight into the η^6 and $\mu_3\text{-}\eta^2\text{:}\eta^2\text{:}\eta^2$ bonding modes in these two different, but strictly related, pairs of isomers.

The pentaruthenium species were studied first. In the first set of calculations, the positional coordinates experimentally obtained from the X-ray studies were used. Next, a naked cluster Ru_5C with bound benzene was considered, and, finally, the complete cluster model with the twelve carbonyl ligands was added. In these models, shown in Chart 1, the symmetry was kept as high as possible for the two isomers and bond lengths were kept constant unless mentioned (further details are in the Appendix).

The total energy obtained in the three situations gives an idea of the usefulness of the models. Another indicator which will be widely employed is the overlap population, which scales as a bond strength. In the present study, besides the overlap population between atoms, the overlap population between fragments will also be presented, as it shows in a more convenient way how the complete benzene molecule, the benzene fragment in this formalism, binds to a metallic fragment, in several conditions. The results are given in Table 1.

It is interesting that the naked clusters and the complete model lead to similar results, namely that the facial isomer is significantly less stable, while the apical and the basal isomers are comparable.

(14) (a) Sirigu, A.; Bianchi, M.; Benedetti, E. *J. Chem. Soc., Chem. Commun.* **1969**, 596. (b) Braga, D.; Grepioni, F.; Dyson, P. J.; Johnson, B. F. G.; Frediani, P.; Bianchi, M.; Piacenti, F. *J. Chem. Soc., Dalton Trans.* **1992**, 2565.

(15) Braga, D.; Grepioni, F.; Parisini, E.; Dyson, P. J.; Blake, A. J.; Johnson, B. F. G. *J. Chem. Soc., Dalton Trans.* **1993**, 2951.

(16) Braga, D.; Grepioni, F.; Dyson, P. J.; Johnson, B. F. G.; Reed, D.; Shepherd, D. S.; Bailey, P. J.; Lewis, J. *J. Organomet. Chem.*, in press.

(17) (a) Farrugia, L. J. *Acta Crystallogr.* **1988**, C44, 997. (b) Mason, R.; Robinson, W. R. *J. Chem Soc., Chem. Commun.* **1968**, 468.

(18) (a) Hoffmann, R. *J. Chem. Phys.* **1963**, *39*, 1397. (b) Hoffmann, R.; Lipscomb, W. N. *J. Chem. Phys.* **1962**, *37*, 2179.

Chart 1

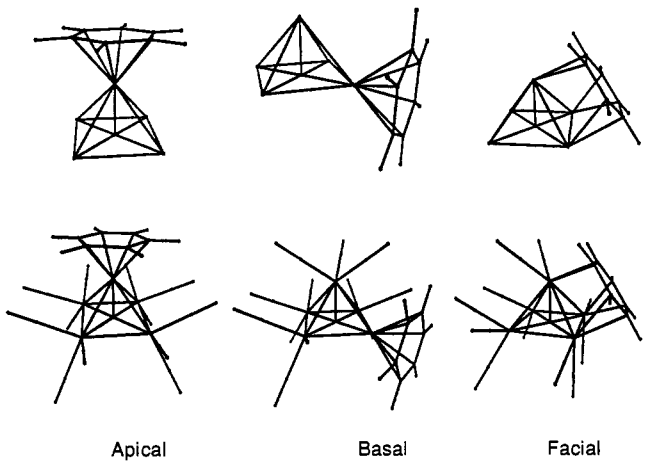

Table 1. Relative Energies (eV) and Overlap Populations[a] between Fragments in Real Molecules and Two Model Clusters, $Ru_5C(C_6H_6)$ and $Ru_5C(CO)_{12}(C_6H_6)$, in Three Geometries, Facial (μ_3-η^2:η^2:η^2), Apical (η^6), and Basal (η^6)

geometry	obsd molecule	$Ru_5C(C_6H_6)$ model	$Ru_5C(CO)_{12}(C_6H_6)$ model
basal-η^6	0.00	0.04	0.00
		0.66	0.64
apical-η^6		0.00	0.16
		0.67	0.69
facial-μ_3	1.90	0.93	0.96
		0.77	0.72

[a] Second rows, models only.

On a qualitative basis, they compare well with the real molecules, where the basal isomer was found to be the most stable. On the other hand, the benzene–cluster bond is consistently stronger for the μ_3-η^2:η^2:η^2 bonding mode than for the η^6 one, as reflected in the larger overlap populations observed. An explanation of this behavior requires a closer look at the molecular orbital diagram. For sake of simplicity and considering the similarity of the results, the Ru_5C cluster and the apical, more symmetric, rather than the basal, geometry will be used. In Figure 3, it is shown how the benzene molecule interacts with Ru_5C in both bonding modes (η^6 on the left, μ_3-η^2:η^2:η^2 on the right).

The π molecular orbitals of benzene are depicted in Figure 4, in a representation, and their symmetry is assigned (in D_{6h}). Their energies are represented in the center of Figure 3.

When coordinating η^6, benzene uses essentially the three occupied π orbitals, a_{2u} and e_{1g}, to donate three pairs of electrons to empty xz, yz and sz, z^2. The cluster orbitals used are mainly localized on the apical Ru atom, as sketched on the left of the diagram. The contribution of the other metal atoms to these levels is in some of the frontier orbitals much smaller, as can be seen in Figure 5. There is some back-donation from occupied xy and x^2-y^2 of the apical ruthenium to the empty e_{2u} set of benzene. Their overlap is very small, as both xy and x^2-y^2 lie parallel to the plane of benzene, and their energies differ by a large amount, which results in the negligible interaction observed. Notice that the $2e_g$ set of benzene σ orbitals hardly mixes in, as their energy is barely unchanged.

Moving now to the other coordination mode, μ_3-η^2:η^2:η^2, it can be seen on the right-hand side of Figure 3 that the diagram is much more complicated, as a consequence of both the lower symmetry allowing mixing between levels and the fact that three metal atoms are necessary to form the bonds. Many more cluster orbitals are involved, but the picture is essentially the same. The benzene molecule was left in the same position as before, but the cluster rotated in order to present a triangular face parallel to the ligand. The highest π orbital of benzene is involved in back-donation, as well as the e_{2u} set. Donation to the metal is achieved by the three occupied π orbitals, a_{2u} and e_{1g}. The bonding orbitals have lower energies than in the previous case, but the energy of the cluster orbitals involved has also changed, making any comparison difficult. The frontier orbitals of Ru_5C which are involved in the most important interactions with each benzene π orbital are represented in Figure 5b. Only the contribution of the Ru atoms in that face is shown, in a view from the top, and the remaining atoms are not depicted in the three-dimensional representation for simplicity. Also, many other orbitals, not shown, mix. The most striking feature, though, is the high energy of the HOMO, which has been pushed up in energy relative to the η^6 case, where it had an almost nonbonding character. In the facial isomer, it is the antibonding combination of a four electron destabilizing interaction involving a_{2u} and a low-energy orbital of Ru_5C, in which another empty orbital of the cluster has mixed in a bonding way, partially relieving that antibonding character. Its very high energy is reflected in the high energy of the isomer.

The interactions between benzene and clusters orbitals are thus different in the two situations, but considering the difficulty of seeing it directly from the interaction diagram, other evidence must be used. One is the overlap population, now decomposed by fragment orbitals. The overlap population between the highest e_{2u} set and all cluster orbitals is small, meaning that it does not participate significantly in bonding for η^6 benzene (and $1b_{1g}$ not at all), though it does for μ_3-η^2:η^2:η^2. As a consequence, the back donation component of bonding is more important for bridging benzene. Similarly, overlap populations between the occupied orbitals of benzene, namely e_{1g} and a_{2u}, are also larger for this geometry. Therefore, there is more benzene to cluster electron donation in this case and, as the components of the bond are stronger, the same happens for the global bonding between fragments. The data given in Table 2, where the occupations of all the benzene π orbitals are indicated, reflect the magnitude of both the ligand to metal donation and metal to ligand back-donation. Recall that for free benzene there are 2 electrons in each of the occupied levels and obviously none in the others. The numbers concerning the two models [$Ru_5C(C_6H_6)$ and $Ru_5C(CO)_{12}(C_6H_6)$] are shown side by side, and once again they are strikingly similar on a qualitative basis.

The occupations are clearly comparable within the two models with one exception, that of the e_{1g} set, which is very much affected by the introduction of the carbonyls, which will compete for the same metal orbitals. The trend is kept, though, showing that for our purpose the simple naked cluster is an acceptable model.

More conclusions can be drawn from the previous results, namely that a more significant increase of C–C bond lengths in benzene is expected for the facial isomer, rather than for the apical one. This arises from both the stronger L → M donation, which depopulates bonding levels, and the stronger M → L back-donation, which populates the C–C antibonding levels. More difficult to derive from the nodal characteristics of the orbitals are the changes in overlap populations between adjacent carbon atoms in the coordinated benzene ring, which decrease from 1.08 in free benzene to 0.85 or 1.00 in the apical isomers of $Ru_5C(C_6H_6)$ and $Ru_5C(CO)_{12}(C_6H_6)$, respectively. On the other hand, when it comes to the facial isomers an alternation of overlap populations starts to be found, as shown in Figure 6, in agreement with the similar alternation observed in bond lengths.

Again, the generalized trend of smaller overlap populations for all isomers reflects the weakening of internal bonds of the ligand and their tendency to become longer. This is a well-known phenomenon, which has been particularly studied in connection with chemical activation of molecules by surfaces.[19] When some molecule binds to a surface (or a cluster), the formation of the new surface–adsorbate or cluster–ligand bonds is usually ac-

(19) (a) Hoffmann, R. *Solids and Surfaces-A Chemist's View of Bonding in Extended Structures*; VCH: Weinheim, Germany, 1988. (b) Hoffmann, R. *Rev. Mod. Phys.* **1988**, *60*, 601.

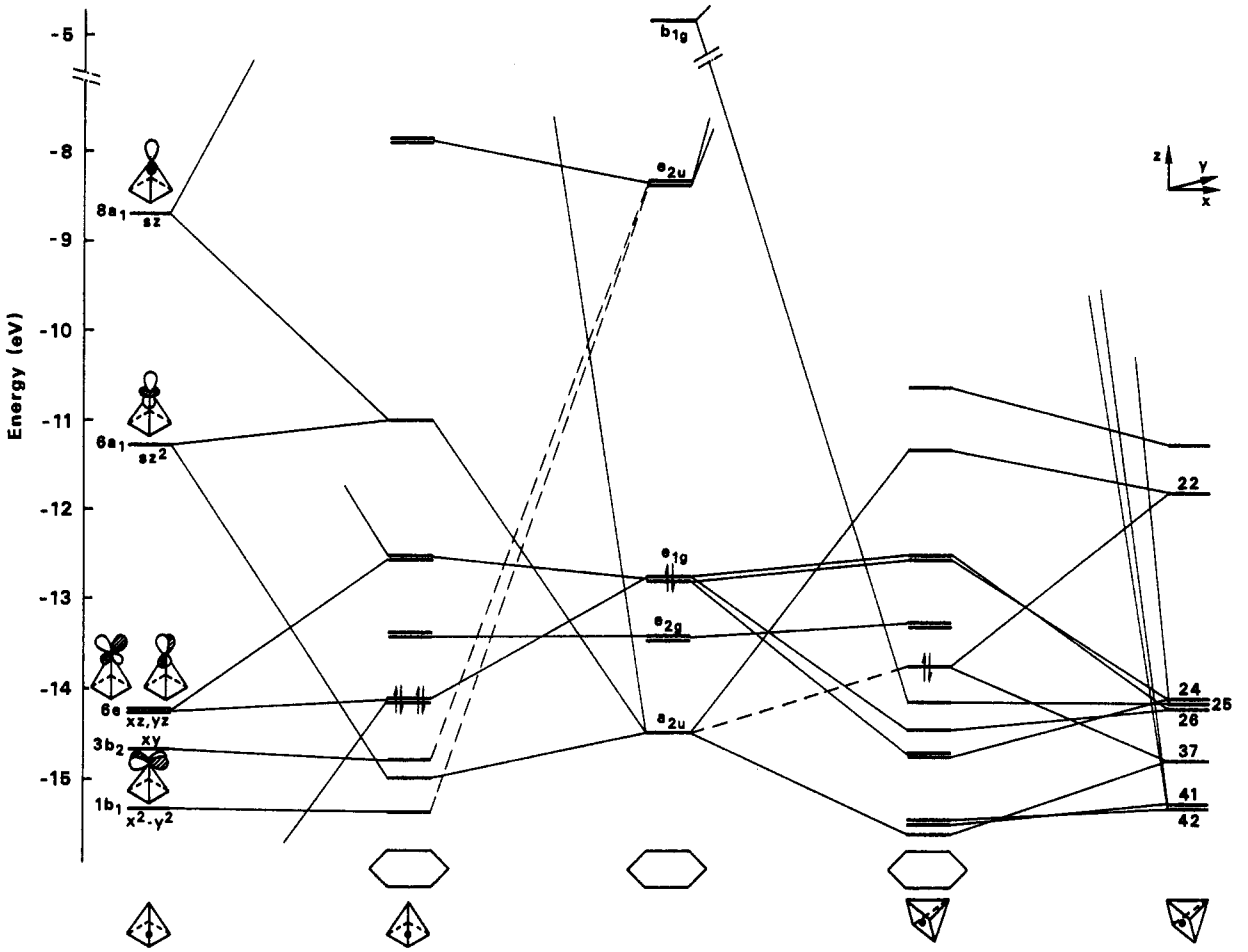

Figure 3. Interaction diagram between benzene and Ru_5C for the η^6 bonding mode (left) and μ_3-η^2:η^2:η^2 (right).

companied by a weakening of the bonds both inside the initial surface or cluster and the coordinated species. In such a context, the important consequence is the enhanced reactivity of the ligand: a weaker bond may be easier to break, thus leading to the production of other derived species. On the other hand, the energetic gain from the formation of the new bonds is partially lost because of the loss of bonding inside each fragment. This explains in a more straightforward way than from the diagram in Figure 3 why the facial isomers, though forming stronger bonds to the clusters, are less stable than the apical or basal ones. The interfragments stronger bond does not compensate for the destruction of considerable more C–C bonding character. It remains to be said that the overlap populations inside the cluster (Ru–Ru, Ru–C, C–O) are comparable and do not appear to play a major role in this balance.

Another matter of interest concerns the deformation of the hydrogens of the μ_3-η^2:η^2:η^2 coordinated benzene ring. Instead of being planar, they are bent out of the plane of the carbon atoms, as referred above, and away from the three ruthenium atoms. Allowing this bending motion to take place led to an energy stabilization of ~0.5 eV for $Ru_5C(C_6H_6)$ and 0.96 eV $Ru_5C(CO)_{12}(C_6H_6)$. The bending angle was found to be close to 20°, slightly less for $Ru_5C(CO)_{12}(C_6H_6)$. The larger stabilization achieved by bending the hydrogen atoms in this latter case results not only from the better overlap between the orbitals of benzene and of the three ruthenium atoms but also from moving them away from the carbonyl oxygens, therefore minimizing the repulsion between them. In what concerns the interaction between fragments, the respective overlap population went up to 0.98 (from 0.72; see Table 1). This increased interaction is also reflected in the occupations of the previously filled (now 1.197, 1.377 for e_{1g}; 1.685 for a_{2u}) or empty levels (now 0.044 for b_{1g}; 0.193, 0.177 for e_{2u}). Both donation and back-donation have increased. The C–C overlap populations have consequently become smaller but keeping their alternate values. There is coincidence between the location of stronger overlap populations calculated and the shorter bonds determined from experimental studies.

There is in the available structures a favored conformation of the benzene ring relative to the Ru_3 face in which three of the C–C bonds (the shortest) eclipse the metal atoms (Chart 2, **e**). Another equally symmetric conformation is observed when the ring rotates 30° (Chart 2, **s**).

The potential energy curve for this rotation is very flat, which has been explained on the basis of the 6-fold symmetry around the benzene ring.[20] In the $Ru_5C(CO)_{12}(C_6H_6)$ cluster, the presence of two carbonyl groups attached to each of the ruthenium atoms in the cluster face is responsible for a small preference for the observed conformation. Indeed, in the absence of carbonyls (simplest model, $Ru_5C(C_6H_6)$) the **s** conformation is more stable by 0.26 eV, while a reverse situation is observed in the complete model cluster, where **s** has an energy higher than **e** by 0.09 eV. In spite of the electronic changes induced in Ru by the extra bonds to the carbonyls, the steric constraints are the determining ones.

Before these Ru_5 clusters are abandoned, there is another interesting problem which we would like to address: the transformation of the basal into the facial isomer.[6] This isomerization is achieved by moving the benzene which is coordinated to one of the ruthenium atoms in the basal plane to a position over the center of the adjacent Ru_3 face and eventually

(20) (a) Hoffmann, R. *Science* **1981**, *211*, 995. (b) Albright, T. A.; Hofman, P.; Hoffmann, R. *J. Amer. Chem. Soc.* **1977**, *99*, 7546. (c) Albright, T. A.; Hoffmann, R.; Tse, Y.; d'Ottavio, T. *J. Am. Chem. Soc.* **1979**, *101*, 3812. (d) Elian, M.; Chen, M. M. L.; Mingos, D. M. P.; Hoffmann, R. *Inorg. Chem.* **1976**, *15*, 1148. (e) Hoffmann, R. *Pure Appl. Chem.* **1978**, *50*, 1.

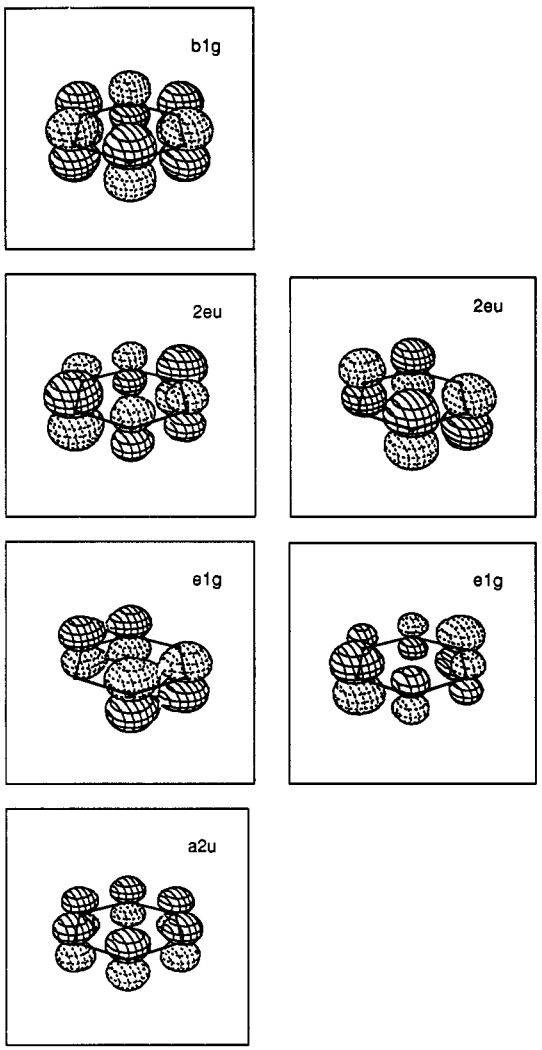

Figure 4. Three-dimensional representation of the π orbitals of benzene.

Table 2. Orbital Occupation of the π Molecular Orbitals of Benzene after Their Interaction with Ru Atoms for Two Model Clusters, $Ru_5C(C_6H_6)$ and $Ru_5C(CO)_{12}(C_6H_6)$, in Two Geometries, Facial (μ_3-η^2:η^2:η^2) and Apical (η^6)

	$Ru_5C(C_6H_6)$		$Ru_5C(CO)_{12}(C_6H_6)$	
benzene orbitals	apical	facial	apical	facial
b_{1g}	0.000	0.035	0.000	0.030
e_{2u}	0.062	0.073	0.072	0.166
	0.061	0.072	0.068	0.152
e_{1g}	0.686	0.461	1.295	1.216
	0.685	0.451	1.295	1.400
a_{2u}	1.823	1.715	1.847	1.742

allowing to hydrogens to bend back. At the same time, two CO groups, one from each of two different Ru atoms, must migrate, while the other two reorientate, as exemplified in Chart 3.

This part of the reorganization of the cluster is more difficult to mimic. It is well-known, though, that carbonyls are very mobile on clusters.[21] For this reason, we decided to use the simple $Ru_5C(C_6H_6)$ model to give an idea of the electronic barrier against movement of the benzene ring across the cluster. In this way, the calculated barrier for the migration is 0.93 eV, dropping to a lower 0.78 eV when the hydrogen atoms are concomitantly allowed to bend back. Such an order of magnitude is compatible with experimental facts.

The Ru_6-based clusters present more structural possibilities as two arene rings can coordinate simultaneously and a larger number of isomers can therefore be expected. Not all of these have been observed until now, as described above. On the other hand, in spite of the same general formula for the family of compounds, they sometimes differ in the topological arrangement of the carbonyls, namely the balance between terminal and bridging ones. As will be discussed in relation to their relative stability, this introduces some difficulties. Two models were also used in this set of calculations, one being the simplest $Ru_6C(C_6H_6)_2$ and the other the complete molecule $Ru_6C(CO)_{11}(C_6H_6)_2$. The isomers which were studied for each are depicted in Chart 4.

The benzene ring binds to the hexaruthenium clusters in essentially the same way as to the Ru_5 for the η^6 and the μ_3-η^2:η^2:η^2 modes. The relative energies of the isomers are given in Table 3, and the greater stability of all species containing η^6 benzene can be noticed.

The first and expected general observation is that the energy becomes lower with the number of η^6 arene rings. The two isomers containing two η^6 rings have comparable energies in the simple model. When it comes to the model with the added eleven carbonyls, they are much more difficult to compare and this explains the two sets of figures given in the Table 3 for what we call here the apical–equatorial (or *cis*) isomer. The first one, corresponding to a lower energy, was obtained with a structure with two bridging and nine terminal carbonyls (observed experimentally in *cis*-$Ru_6C(CO)_{11}(\eta^6$-$C_6H_3Me_3)(\eta^6$-$C_6H_6)$,[4b] while the second one obtained, with one bridging and ten terminal carbonyls, as seen experimentally in *cis*-$Ru_6C(CO)_{11}(\eta^6$-C_6H_4-$Me_2)(\eta^6$-$C_6H_5Me)$,[22] corresponds to a higher energy. Having found that extended Hückel calculations are not very good in describing accurately the energetic balance between terminal and bridging carbonyls, which are known from experimental studies to be very fluxional, we think that these numbers should not be taken at face value. Also, there is a continuum of geometries between a strictly linear terminal and a perfect bridging carbonyl, with all the asymmeric bonding modes in between.[23] Furthermore, the precursor $Ru_6C(CO)_{17}$ is known in *three* different structural forms in the solid state, differing for the pattern of symmetric and asymmetric brigding ligands, and in the rotameric conformation of the apical tricarbonyl units.[14] For all these reasons and the experience with the Ru_5C clusters, we might recall the numbers concerning the naked cluster and decide that the two isomers are likely to have similar energies. The other bis-facial geometries were both found to be high-energy species in the absence of the carbonyl groups. The uncertainty about how to distribute them around the cluster would again result in a range of different possible structural types with different energies, so we did not even attempt at building them. From the two possibilities, the trans would probably allow a better distribution of carbonyls and less steric constraints.

Though each benzene binds to the cluster in the same way as described for the pentaruthenium clusters, the new factor in this new series of compounds is the competition between two benzene rings for the metal orbitals. As expected, no difference exists between the two arene rings when each binds to only one metal atom, the octahedron being a regular polyhedron (though the same may not be true for the complete environment including carbonyls). On the other hand, the coexistence of the two bonding types in the same molecule allows us to compare their bonding situation when competing.

The results are those to be expected. Going back to the fragment decompostion formalism, we consider now three fragments in the apical–facial Ru_6C cluster: Ru_6C, the apical

(21) (a) Aime, S.; Milone, L. *Prog. Nucl. Magn. Reson. Spectrosc.* **1977**, *11*, 183. (b) Cotton, F. A.; Hanson, B. E. *Rearrangements in Ground and Excited States*; De Mayo, P., Ed.; Academic Press: New York, 1980; p 379. (c) Evans, J. W. *Adv. Organomet. Chem.* **1979**, *16*, 319. (d) Faller, J. W. *Adv. Organomet. Chem.* **1978**, *16*, 21. (e) Johnson, B. F. G.; Benfield, R. E. *Transition Metal Clusters*; Johnson, B. F. G., Ed.; Wiley: New York, 1980, p 471.

(22) Braga, D.; Grepioni, F.; Dyson, P. J.; Johnson, B. F. G. To be published.

(23) Sironi, A. *Inorg. Chem.* **1992**, *31*, 2467.

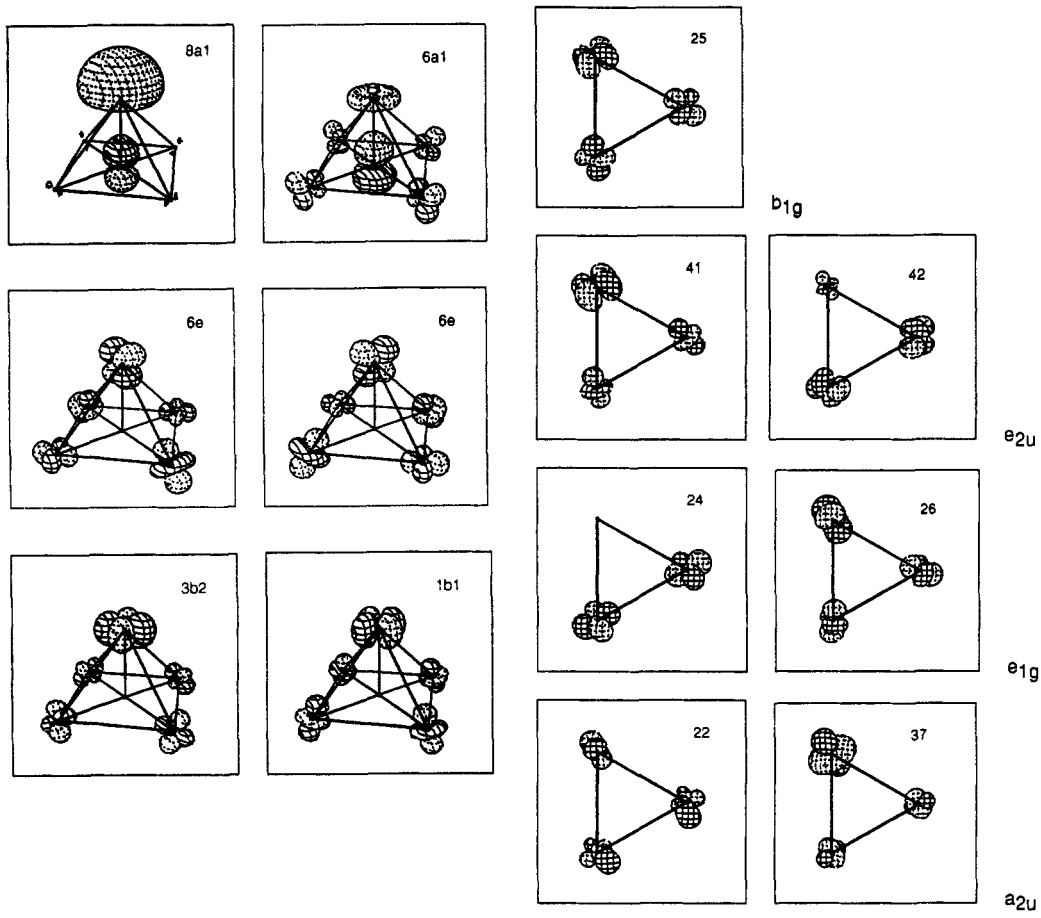

Figure 5. Three-dimensional representation of the frontier orbitals of the Ru_5C model structure (a) having a large contribution from the apical Ru atom and (b) being mainly localized on the Ru_3 face.

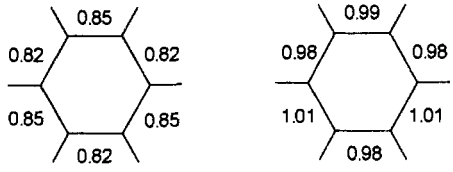

Figure 6. C–C overlap populations of coordinated benzene for the μ_3-η^2:η^2:η^2 coordination mode: $Ru_5C(C_6H_6)$ model (left) and $Ru_5C(CO)_{12}(C_6H_6)$ model (right).

Chart 2

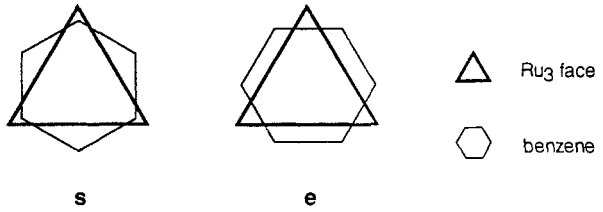

benzene and the facial benzene. The cluster fragment has an overlap population of 0.63 with the facial ligand and 0.61 with the apical one. Bonds between facial benzene and the Ru_3 face are still the strongest. The occupations of the fragment orbitals after coordination are only slightly different from those in Table 2, and there is no reason to repeat them. The facial ligand is a better donor, and in spite of being also a better acceptor and recovering some electrons through back-donation, there is an overall larger positive charge in it than in the η^6 coordinated benzene ring.

Crystal Structure of Arene Clusters. The molecular structure of flexible molecules in the solid state is not necessarily identical to that in solution or in the gas phase, since crystal forces, *i.e. intermolecular bonding*, can give a significant contribution to the definition of the global energy of the system.[24] As pointed out above, arene clusters are extremely flexible structural systems since arene reorientation and isomerization combines with CO scrambling over the cluster framework. In these cases the environment, whether constituted of the same molecule packed in an ordered way in the crystal structure or by rapidly tumbling solvent molecules in solution, is not simply a spectator but can have great influence on the structural features that are observed by crystallographic or spectroscopic techniques.

Chart 3

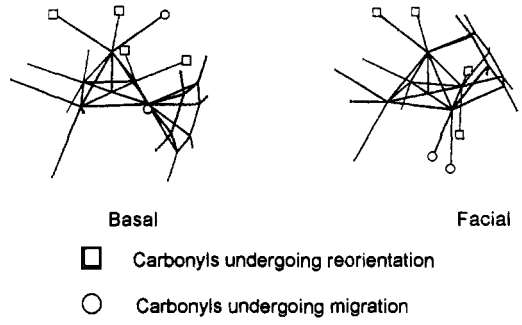

In this section we focus on the interplay between molecular and crystal structures of the arene clusters discussed above.

The observed crystal structures have been *decoded* by studying the distribution and interaction of the first neighboring molecules among the molecules surrounding the one chosen as reference. Empirical packing potential energy calculations within the pairwise atom–atom approach[25] and packing analysis based on graphical methods[26] have been used to this purpose. These

(24) (a) Braga, D. *Chem. Rev.* **1992**, *92*, 633. (b) Braga, D.; Grepioni, F. *Acc. Chem. Res.* **1994**, *27*, 51.

Chart 4

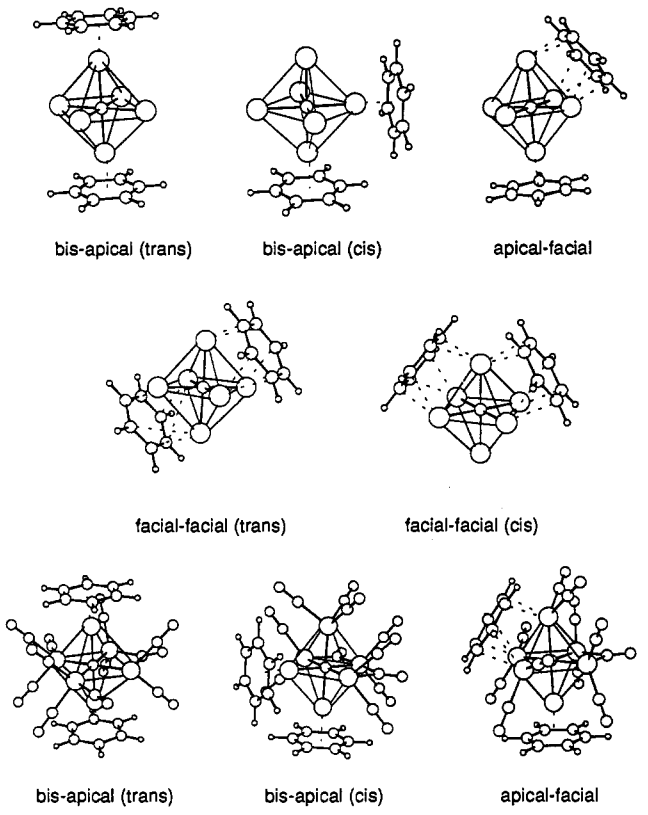

Table 3. Relative Energies (eV) of Real Molecules and the Two Models $Ru_6C(C_6H_6)_2$ and $Ru_6C(CO)_{11}(C_6H_6)_2$ for Several Possible Isomers

geometry	real molecule	$Ru_6C(C_6H_6)_2$	$Ru_6C(CO)_{11}(C_6H_6)_2$
bis-apical *trans*	0.00	0.12	0.00
bis-apical *cis*		0.00	−0.49 to +0.47
apical–facial	2.35	0.96	0.56
bis-facial *trans*		2.02	
bis-facial *cis*		1.87	

methods have been shown to yield an accurate knowledge of the immediate molecular environment and of the intermolecular interlocking. Furthermore, a (rough) estimate of the packing potential energy (ppe) can be obtained (see methodology below).[25] The efficiency of volume occupation in the crystal is represented by the value of the packing coefficient (pc), which can be evaluated from the relationship $pc = V_{mol}\cdot Z/V_{cell}$, where V_{mol} represents the van der Waals molecular volume. The volumes have been estimated with the integration method put forward by Gavezzotti.[27]

All crystal structure parameters relevant for the following discussion are grouped in Table 4.

Partitioning of the ppe into the separate contributions of all first neighboring molecules allows one to detect specific intermolecular interactions. In particular, the appearance of intermolecular *repulsions* between H atoms and surrounding O atoms belonging to carbonyl groups is diagnostic of the presence in the crystal lattice of hydrogen bonds of the C–H··O type.[28] These interactions have been demonstrated to play a significant role in the crystal packing of organic molecules.[29] Their importance in crystalline organometallic cluster systems is increased by the presence of a large number of CO groups. As shown in Table 4, *short* (<2.45 Å) C–H··O intermolecular interactions are evident *only* in crystals of the species carrying apical benzene (see also below).

With respect to Table 4 the following general considerations can be made:

(i) The molecular volumes (V_{mol}) are in both Ru_5 and Ru_6 clusters slightly larger for the apical (425.1 and 495.0 Å^3) than for the facial isomers (416.8, and 489.5 Å^3). This very likely reflects the fact that the benzene ligands in the facial mode of bonding are more deeply embedded within the CO-ligand shell than when apically bound.

(ii) Packing coefficients fall in a fairly narrow range (0.69–0.73). The most dense molecular arrangement is present in crystalline $Ru_6C(CO)_{11}(\mu_3\text{-}\eta^2\text{:}\eta^2\text{:}\eta^2\text{-}C_6H_6)(\eta^6\text{-}C_6H_6)$ (see also below). These values are strictly comparable with those of organic molecules and of organometallic mononuclear systems containing carbonyl ligands and arenes.[30]

(iii) As expected, ppe is more cohesive for the larger hexanuclear than for the pentanuclear species. Less predictable, however, is the fact that the crystals of the hexanuclear apical–facial species are more cohesive than the bis-apical species ($\Delta = 8.0$ kcal·mol^{-1}), whereas the crystals of the two pentanuclear species have comparable cohesive energy. The difference *in favor* of the apical–facial isomers is maintained if other potential parameters are used. It is important to appreciate that, although atom–atom pairwise potential energy calculations for such complex crystal systems are bound to yield only very approximate values of the packing energies, differences between values calculated with the same choice of potential parameters are more reliable.

(iv) Atom–atom pairwise potential energy calculations allow partitioning of the ppe over the separate contributions of specific atomic groupings to the total cohesive energy. Table 4 shows that, irrespective of the cluster nuclearity and of the type of coordination, the contribution of benzene falls in the narrow range −16.4 to −18.3 kcal·mol^{-1} accounting for between 15 and 18% of the total ppe.

(v) The contribution to ppe of the *direct* arene–arene interactions, on the other hand, reflects the specificity of the packing patterns (see below). In the hexanuclear bis(benzene) species, where there is graphitic pairing of the benzene ligands belonging to neighboring molecules, the interaction between benzene moieties, irrespective of the mode of coordination, is of *ca.* 4.8 kcal·mol^{-1}. This interaction is much smaller in the pentanuclear mono(arene) species. It is worth noting, however, that the strongest benzene–benzene interaction is between the two independent molecules present in the asymmetric unit of crystalline $Ru_5C(CO)_{12}(\eta^6\text{-}C_6H_6)$ (−2.6 kcal·mol^{-1}).

We can now proceed to a detailed examination of the intermolecular interlocking within the crystal structures.

The packing of $Ru_5C(CO)_{12}(\eta^6\text{-}C_6H_6)$ is characterized by the presence of two independent molecules (A and B). The two molecules are essentially identical in their molecular structures, differing only in the rotameric orientation of the apical benzene fragment with respect to the cluster. As shown in Table 4, short intermolecular contacts of the C–H(benzene)··O type involve the hydrogen atoms of the benzene ligand belonging to A and two oxygen atoms belonging to two different molecules of type B. Hence, these interactions preferentially link together the two independent molecular units.

The crystal structure of $Ru_5C(CO)_{12}(\mu_3\text{-}\eta^2\text{:}\eta^2\text{:}\eta^2\text{-}C_6H_6)$ can be described as formed by adjacent molecular piles. The benzene

(25) (a) Kitaigorodsky, A. I. *Molecular Crystals and Molecules*; Academic Press: New York, 1973. (b) Gavezzotti, A.; Simonetta, M. *Chem. Rev.* **1981**, *82*, 1. (c) *Organic Solid State Chemistry*; Desiraju, G. R., Ed.; Elsevier: Amsterdam, 1987. (d) Desiraju, G. R. *Crystal Engineering. The Design of Organic Solids*; Elsevier: Amsterdam, 1989.

(26) Keller, E. SCHAKAL93, Graphical Representation of Molecular Models. University of Freiburg, FRG.

(27) Gavezzotti, A. *J. Am. Chem. Soc.* **1989**, *111*, 1835.

(28) (a) Braga, D.; Grepioni, F.; Parisini, E.; Johnson, B. F. G. J.; Martin, C. M.; Nairn, J. G. M.; Lewis, J.; Martinelli, M. *J. Chem. Soc., Dalton Trans.* **1993**, 1891. (b) Braga, D.; Grepioni, F. *J. Chem. Soc., Dalton Trans.* **1993**, 1223.

(29) Desiraju, G. R. *Acc. Chem. Res.* **1991**, *24*, 290.

(30) Braga, D.; Grepioni, F. *Organometallics* **1991**, *10*, 2563. Braga, D.; Grepioni, F. *Organometallics* **1992**, *11*, 711.

Table 4. Comparison of Relavant Crystal Packing Parameters

param	compound			
	$Ru_5C(CO)_{12}(\eta^6\text{-}C_6H_6)$	$Ru_5C(CO)_{12}(\mu_3\text{-}C_6H_6)$	$Ru_6C(CO)_{11}(\eta^6\text{-}C_6H_6)_2$[b]	$Ru_6C(CO)_{11}(\eta^6\text{-}C_6H_6)(\mu_3\text{-}C_6H_6)$
V_{cell} (Å^3)	4811.96[a]	1204.09	2812.72	1350.31
V_{mol} (Å^3)	425.1[a]	416.8	495.0	489.5
packing coeff	0.71	0.69	0.70	0.73
ppe (kcal·mol^{-1})	-97.3[a]	-96.8	-106.3	-114.2
short C–H··O contacts (Å)	O(7A)··H(14B), 2.38; O(4B)··H(17A), 2.27		O(13)··H(54), 2.44	
benzene contribn to ppe[b] (kcal·mol^{-1})	η^6(A), -17.31; η^6(B), -17.63; η^6(av), -17.47	μ_3, -16.44	$\eta^6(1) = \eta^6(2)$,[b] -16.7	η^6, -18.27; μ_3, -16.70
benzene–benzene interaction (kcal·mol^{-1})	η^6(A)–η^6(A), -0.38; η^6(A)–η^6(B), -0.19; η^6(A)–η^6(B), -2.55	μ_3–μ_3, -1.05	$\eta^6(1)$–$\eta^6(1) = \eta^6(2)$–$\eta^6(2)$, -0.81; $\eta^6(1)$–$\eta^6(2)$, -4.80	η^6–η^6, -4.81; μ_3–μ_3, -4.75; η^6–μ_3, -0.68

[a] Obtained as mean values averaged over the two independent molecules present in the asymmetric unit (A, B). [b] The two apical benzene rings are identified as $\eta^6(1)$ and $\eta^6(2)$.

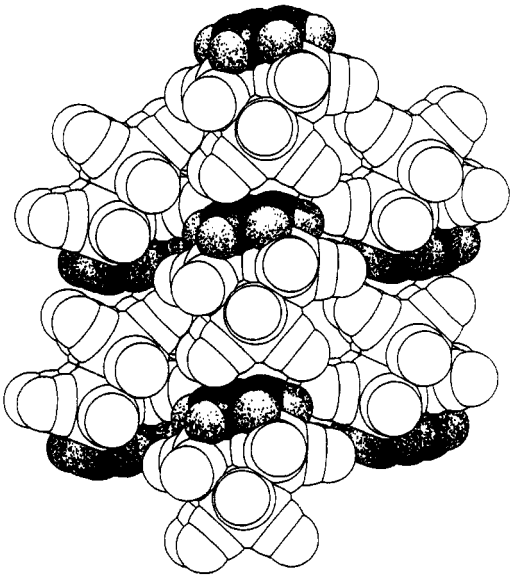

Figure 7. Molecular piles in crystalline $Ru_5C(CO)_{12}(\mu_3\text{-}\eta^2\text{:}\eta^2\text{:}\eta^2\text{-}C_6H_6)$.

ring of one molecule along the pile interacts directly with a tetracarbonyl unit (constituted by two radial and two axial CO groups bonded to one basal edge of the cluster pyramid) of a neighboring molecule. Each pile is surrounded by other six piles, four of which placed in antiparallel direction with respect to the central one as shown in Figure 7. This packing motif is very similar to that observed in crystals of other mono(arene) derivatives of the type $Ru_6C(CO)_{14}(\eta^6\text{-arene})$ (arene = C_6H_6, $C_6H_3Me_3$, $C_6H_4Me_2$) and in the crystal of the only example of a facial mono(arene) cluster so far characterized, namely $Ru_6C(CO)_{14}(\mu_3\text{-}\eta^2\text{:}\eta^2\text{:}\eta^2\text{-}C_{16}H_{16})$. Furthermore, there is a pronounced analogy with the packing of arene mononuclear systems like $(\eta^6\text{-}C_6H_6)M(CO)_3$ and $(\eta^6\text{-}C_6Me_6)M(CO)_3$ (M = Cr, Mo), which arrange themselves in the solid forming exactly the same kind of pattern.[30] In the case of mononuclear systems this has been attributed to the near cylindrical shape of molecules formed by disklike benzene and hexamethylbenzene fragments together with conical tricarbonyl units. When the molecular shape deviates from cylindrical (as when the ligand is toluene, durene, or xylene) different packing patterns are observed.[24] In crystalline $Ru_5C(CO)_{12}(\mu_3\text{-}\eta^2\text{:}\eta^2\text{:}\eta^2\text{-}C_6H_6)$ the facial benzene lies on a flat fragment defined by six radial ligands which form a fairly regular hexagon parallel to the ring plane. This fragment is, therefore, identical to that present in the trinuclear clusters $M_3(CO)_9(\mu_3\text{-}\eta^2\text{:}\eta^2\text{:}\eta^2\text{-}C_6H_6)$ (M = Ru, Os).

The isomeric pair of bis(benzene) clusters $Ru_6C(CO)_{11}(\eta^6\text{-}C_6H_6)(\mu_3\text{-}\eta^2\text{:}\eta^2\text{:}\eta^2\text{-}C_6H_6)$ and $Ru_6C(CO)_{11}(\eta^6\text{-}C_6H_6)_2$ has been studied in detail. Although the crystal structure of the facial–apical isomer has already been investigated, it is worth recalling in the context of this discussion its main features in comparison

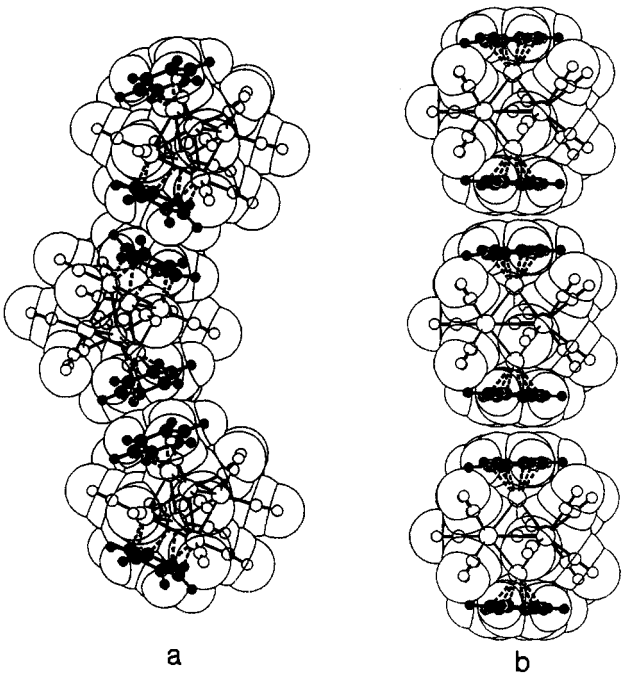

Figure 8. The molecular "snakes" and piles present in crystalline $Ru_6C(CO)_{11}(\eta^6\text{-}C_6H_6)(\mu_3\text{-}\eta^2\text{:}\eta^2\text{:}\eta^2\text{-}C_6H_6)$ and $Ru_6C(CO)_{11}(\eta^6\text{-}C_6H_6)_2$, respectively.

with those of crystalline $Ru_6C(CO)_{11}(\eta^6\text{-}C_6H_6)_2$. In the case of $Ru_6C(CO)_{11}(\eta^6\text{-}C_6H_6)(\mu_3\text{-}\eta^2\text{:}\eta^2\text{:}\eta^2\text{-}C_6H_6)$ the molecule does not self-assemble in a close-packed arrangement. The reference molecule interacts with two next-neighboring molecules generated by crystallographic centers of symmetry forming molecular "snakes" through the crystal structure (see Figure 8a). The separation between the carbon rings is 3.29 and 3.56 Å, *i.e.* strictly comparable to graphite itself. The molecules of $Ru_6C(CO)_{11}(\eta^6\text{-}C_6H_6)_2$ organize themselves in their crystal with benzene ligands facing each other along the *a*-axis direction thus forming beautiful molecular piles "linked" via benzene–benzene interactions (see Figure 8b). Each pile is surrounded by other six piles. The C_6H_6 ring planes on each molecule are almost parallel, the angle between them being only 4.0°. The distance between the two C_6H_6 ring planes is 3.52 Å, which is in the range (3.4–3.5 Å) commonly observed for arene–arene interactions in this family of crystalline complexes. The bridging carbonyl interacts on one side with two arene rings of the adjacent pile (see Figure 9).

The nature of the intermolecular interactions between benzene rings in adjacent molecules along one of these chains was probed by running an extended Hückel calculation (with the tight-binding approach[31]) in one of these chains from which the carbonyls were removed, owing to the size of the problem and having in mind that the naked cluster has been a helpful model when looking

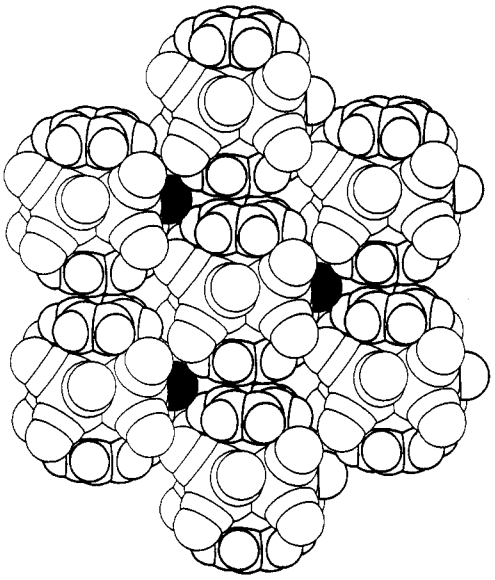

Figure 9. Bridging carbonyl interacting on one side with two arene rings of the adjacent piles in crystalline $Ru_6C(CO)_{11}(\eta^6\text{-}C_6H_6)_2$.

at what happens in the benzene rings. Overlap populations were calculated between pairs of atoms belonging to different molecules and having the shortest contacts. Very small but positive overlap populations were found between two pairs of carbon atoms in adjacent benzene rings, suggesting the existence of very weak bonds. These became stronger when approaching the chain elements and disappeared when they were moved away, in the appropriate behavior of a covalent bond.

Conclusions

With this paper we have attempted to address the perpetual steric–electronic dualism that pervades the structural chemistry of flexible molecular systems.

The intramolecular bonding in the two pairs of arene cluster isomers has been tackled by molecular orbital extended Hückel calculations. The main outcomes of this part of the study can be summarized as follows:

(i) Extended Hückel molecular orbital calculations recognize the correct order of molecular stability, *viz.* the apical isomers, whether in pentanuclear mono(arene) adducts or in bis(arene) hexanuclear systems are the most stable isomeric forms. This is in agreement with the observation that apical isomers are always the final product of the reaction and subsequent interconversion process.

(ii) On ideal passage from apical to facial bonding, the energetic gain from the formation of the new bonds is partially lost because of the larger loss of bonding inside each fragment. As a consequence, the facial isomers, though forming stronger bonds to the clusters, are less stable than the apical ones because the interfragments stronger bond does not completely compensate for the destruction of considerable more C–C bonding character.

(iii) The calculations show that in $\mu_3\text{-}\eta^2\text{:}\eta^2\text{:}\eta^2$ coordinated benzene rings the hydrogens atoms should bent out of the plane of the carbon atoms, as this leads to stronger benzene–cluster bonds.

The intermolecular bonding and the molecular organization in the crystal structures have been investigated by atom–atom packing potential energy calculations. The results can be summarized as follows:

(iv) In terms of crystal cohesion, the crystals containing facial isomers appear to be as cohesive as—if not more cohesive than—those formed by the apical isomers. This result does not depend on the choice of atom–atom potential parameters and does not change if the "additional stabilization" of the C–H···O hydrogen bonds is taken into account (see below).

(v) Intermolecular hydrogen bonds of the C–H···O type are established preferentially between apical arenes and CO ligands. Whether this is due to an electronic reason, *viz.* H atoms in apical benzene being more electropositive than in facial benzene, is difficult to say. The extended Hückel calculations described above give extremely small charge differences between hydrogen atoms of the two isomers and cannot, therefore, discriminate among such subtle electronic effects. It is also possible that the facial ligands, being deeply embedded in the cluster ligand shell, are more "screened" from the CO ligands than apical ones.

(vi) Bis(benzene) clusters self-organize in their crystal structures by preferentially grouping together the arene fragments. In spite of the dramatic difference in molecular structures between the two bis(benzene) species there is a stringent analogy between the "snakes" present in crystalline $Ru_6C(CO)_{11}(\eta^6\text{-}C_6H_6)(\mu_3\text{-}\eta^2\text{:}\eta^2\text{:}\eta^2\text{-}C_6H_6)$ and the molecular piles in crystalline $Ru_6C(CO)_{11}(\eta^6\text{-}C_6H_6)_2$. Molecular piles are also the fundamental packing motif in crystalline $Ru_5C(CO)_{12}(\mu_3\text{-}\eta^2\text{:}\eta^2\text{:}\eta^2\text{-}C_6H_6)$, while preferential, C–H···O hydrogen-bound, molecular pairs form the packing unit in crystalline $Ru_6C(CO)_{12}(\eta^6\text{-}C_6H_6)$.

Although great care should be exercised in relating the results of the two types of calculations employed in this paper, it is noteworthy that both methods have retraced the known chemical behaviors, *viz.* that facial isomers are always formed first (very likely for kinetic reasons) and undergo conversion to the more stable apical isomers. The facial isomers are sufficiently stable, though, as to allow separate crystallization and characterization. The method is also able to discriminate between *trans*- and *cis*-isomers indicating that this latter isomer is favored. While *cis*-isomers are known for some mixed-arene crystals, the existence of a bis(benzene) cluster in a *cis*-arrangement awaits to be experimentally confirmed. While our results do not permit an absolute scale of cohesive energy within the various crystal structures, they certainly demonstrate that less stable molecular structures can be isolated if crystal cohesion can compensate for the energetic unbalance. It should be stressed, on closing, that these are only initial (hence—admittedly—uncertain) steps toward a deeper understanding of the relationship between the structure observed in the solid state, which is a subtle compromise between intra- and intermolecular bonding, and the structure of the (often hypothetical) "gas-phase" isolated molecular unit.

Acknowledgment. D.B., F.G, and M.J.C. acknowledge the CNR (Italy) and JNICT (Portugal) for joint financial support. D.B., F.G., and B.F.G.J. thank NATO for a travel grant. P.J.D. thanks the SERC and British Petroleum for financial support.

Appendix

All the calculations were done using the extended Hückel method[13] with modified H_{ij}'s[32] and the tight-binding approach for the unidimensional chain.[31] The basis set for the metal atom consisted of *n*s, *n*p, and (*n* – 1)d orbitals. The s and p orbitals were described by single Slater-type wave functions, and the d orbitals were taken as contracted linear combinations of two Slater-type wave functions. Standard parameters were used for C and H, while those for Ru were as follows (H_{ii}/eV, ζ): 5s, –10.40, 2.078; 5p, –6.89, 2.043; 4d, –14.90, 5.378, 2.303 (ζ_2), 0.5340 (c_1), 0.6365 (c_2). Three-dimensional representations of orbitals were drawn using the program CACAO.[33]

In all calculations, except where explicitly mentioned, idealized models were used, based on the experimentally observed structures. The Ru_6C cluster was an octahedron with the carbon atom in the center, and the Ru_5C cluster was obtained from it by removing one Ru atom. The positions of the carbonyl ligands around Ru atoms were as close as possible to the

(31) (a) Wangbo, M.-H.; Hoffmann, R. *J. Am. Chem. Soc.* **1978**, *100*, 6093. (b) Wangbo, M.-H.; Hoffmann, R.; Woodward, R. B. *Proc. R. Soc. London* **1979**, *A366*, 23.

(32) Ammeter, J. H.; Bürgi, H.-B.; Thibeault, J. C.; Hoffmann, R. *J. Am. Chem. Soc.* **1978**, *100*, 3686.

(33) Mealli, C.; Proserpio, D. M. *J. Chem. Educ.* **1990**, *67*, 39.

experimental ones, but some angles were optimized in the case of facial isomers. The $Ru(CO)_3$ fragment was taken as a half-octahedron. The following distances were used (Å): Ru–Ru, 2.89; Ru–C(CO), 1.89; Ru–C(benzene), 2.22; C–C, 1.40; C–H, 1.08; C–O, 1.13.

Packing potential energy calculations were performed within the atom–atom pairwise potential energy method. Use was made of the expression $ppe = \Sigma_i\Sigma_j[A \exp(-Br_{ij}) - Cr_{ij}^{-6}]$, where ppe represents the packing potential energy and r_{ij} the nonbonded atom–atom intermolecular distance. Index i in the summation runs over all atoms of the reference molecule, and index j, over the atoms of the surrounding molecules or ions within a preset cutoff distance (usually 15 Å with large cluster systems). The ruthenium atoms were attributed the potential coefficients available for argon.[34] Two sets of potential energy parameters for carbon and oxygen were used and the results compared; the first set (named MRK) is the one put forward by Mirsky,[34a] while the second set contains the generalized parameters obtained by Gavezzotti and Filippini (set named GVF).[34b] These parameters are reported in the supplementary table. Since the two sets of potential parameters yield similar results, only those presented via GVF are discussed in the text.

The molecular volumes (V_{mol}, V_{anion}, V_{cation}) were calculated by using literature van der Waals radii for main-group elements and an arbitrary radius of 2.35, 1.75, 1.50, and 1.17 Å for the Ru, C, O, and H atoms, respectively. V_{mol} values were obtained with the integration model.[27] In the case of high-nuclearity carbido–carbonyl clusters this method yields values that are more "accurate" than those obtained with the Kitaigorodky "intersecting cups" model. This latter model has been successfully employed in many instances to estimate the molecular volumes of less crowded cluster molecules.[35] Problems have been seen to arise when interstitial atoms are present such as in the systems under examination. The volumes calculated with the integration steps method are invariably found larger than those calculated with the "intersecting cups" method. It is important to stress, however, that, although the actual values depend on the model employed, the relative ratio between the diverse values obtained for the different molecules is preserved irrespective of the method used for the volume calculation. The calculation procedures of V_{mol} and pc, as well as that of ppe, are all implemented within Gavezzotti's OPEC suite of programs.[36]

Supplementary Material Available: A table of packing potential energy parameters (1 page). Ordering information is given on any current masthead page.

(34) Braga, D.; Grepioni, F. *Acta Crystallogr., Sect. B* **1989**, *B45*, 378. Braga, D.; Grepioni, F.; Milne, P.; Parisini, E. *J. Am. Chem. Soc.* **1993**, *115*, 5115. Braga, D.; Grepioni, F. *J. Chem. Soc., Dalton Trans.* **1993**, 1223.

(35) (a) Mirsky, K. *Procedings of the International Summer School on Crystallographic Computing*; Delft University Press: Twente, The Netherlands, 1978; p 169. (b) Gavezzotti, A.; Filippini, G. *Acta Crystallogr., Sect B*, in press.

(36) Gavezzotti, A. OPEC. University of Milano, 1983. See also: Gavezzotti, A. *J. Am. Chem. Soc.* **1983**, *195*, 5220.